ISSN 0023-1584, Kinetics and Catalysis, 2006, Vol. 47, No. 2, pp. 310–325. © MAIK "Nauka/Interperiodica" (Russia), 2006.

Modeling Ethylene and Propylene Homopolymerization by Late-Transition-Metal Catalysts: A Combined Quantum Mechanical and Stochastic Approach[1]

A. Michalak[a,b] and T. Ziegler[b]

[a] *Department of Chemistry, University of Calgary, Calgary, Alberta, Canada T2N 1N4*
[b] *Department of Theoretical Chemistry, Jagiellonian University, Cracow, Poland*
e-mail: Ziegler@ucalgary.ca

Received July 11, 2005

Abstract—In the present account, we describe how it is possible to model alkene homopolymerization in processes catalyzed by late-transition-metal complexes in such a way as to predict the influence of the catalyst structure and the reaction conditions (temperature and olefin pressure) on the polyolefin microstructure. Gradient corrected DFT has been used to determine the energetics and the activation barriers of the elementary reactions in these processes. A stochastic model has been developed and employed in order to simulate the polymer growth under different T and p conditions.

DOI: 10.1134/S0023158406020248

INTRODUCTION

Brookhart and coworkers [1–4] have recently developed Ni(II) and Pd(II) diimine-based catalysts of the type (ArN=C(R)–C(R)=NAr)M–CH_3^+ (**1a** in Fig. 1) that are promising alternatives to both Ziegler–Natta systems and metallocene catalysts for olefin polymerization. Not only can these catalysts convert ethylene into high-molecular-weight polyethylene, but the polymers also exhibit a controlled level of short chain branching. Traditionally, such late-metal catalysts are found to produce dimers or extremely low molecular weight oligomers owing to a facile chain termination processes [5, 6]. It should be pointed out that cationic Pd(II) complexes containing bidentate tertiary phosphine ligands already were developed in the early 1980s by Sen [5] and Drent [6] as catalysts for the copolymerization of CO and ethylene.

Brookhart's group has studied the mechanistic details of the polymerization, including the role of the bulky substituents on the diimine ligands [1–7]. Three main processes are thought to dominate the polymerization chemistry of these catalyst systems, namely, propagation, chain branching, and chain termination (Fig. 2). Following cocatalyst activation of the precatalyst, a diimine methyl cation is formed. The first insertion of ethylene yields a diimine alkyl cation which upon uptake of another ethylene molecule produces a metal alkyl olefin π-complex. This π-complex has been established by NMR studies [1–4] to be the catalytic resting state of the system. The chain propagation cycle is depicted in Fig. 2, stage (a). The first step involves the insertion of the coordinated olefin moiety to form a metal alkyl cationic species. Rapid uptake of monomer returns the system to the initial resting state π-complex. Chain termination occurs via monomer-assisted β-hydrogen elimination, either in a fully concerted fashion as illustrated in Fig. 2, stage (b), or in a multistep associative mechanism as implicated by Johnson et al. [1].

The unique short chain branching observed with these catalysts is proposed to occur via an alkyl chain isomerization process as sketched in Fig. 2, stage (c). In this proposed process, β-hydride elimination first yields a putative hydride olefin π-complex. Rotation of the π-coordinated olefin moiety about its coordination axis, followed by reinsertion, produces a secondary carbon unit and therefore a branching point. Consecutive repetitions of this process allows the metal center to migrate down the polymer chain, thus producing longer chain branches.

Similar Ni and Pd catalysts developed by Keim [8] and others [9, 10] which do not possess the bulky ligand systems have been used to produce dimers or extremely low molecular weight oligomers. Brookhart has suggested [1–3] that the bulky aryl ligands act to preferentially block the axial sites of the metal center as illustrated by Fig. 3. This feature in the catalyst system must in some way act to retard the chain termination process relative to the propagation process, thereby allowing these catalysts to produce high-molecular-weight polymers.

More recently, the groups of Brookhart [11] and Gibson [12] investigated the catalytic potential of iron(II) and cobalt(II) complexes with tridentate pyri-

[1] The text was submitted by the authors in English.

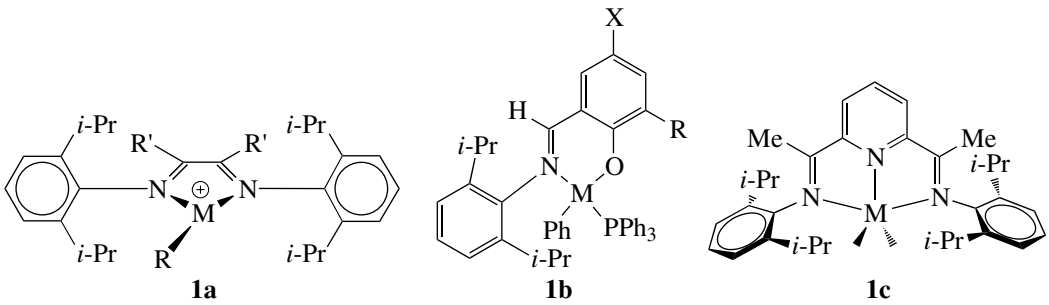

Fig. 1. Late-transition-metal catalysts for olefin polymerization of current interest.

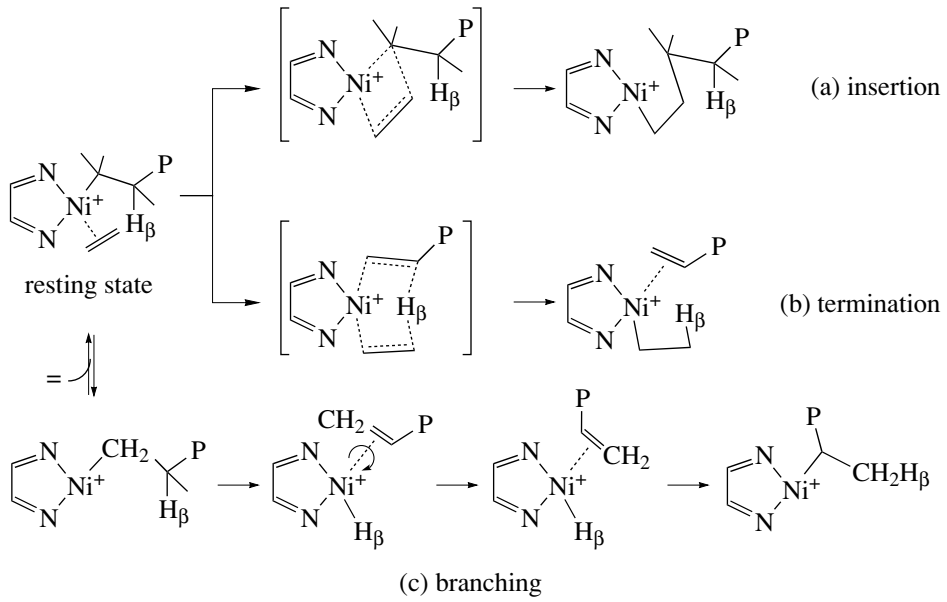

Fig. 2. Proposed reaction mechanism for (a) insertion, (b) chain termination, and (c) chain branching in the case of the Brookhart Ni-bisimine polymerization catalyst. Large bulky substituents have been removed for clarity.

dine diimine ligands (**1c** in Fig. 1). They found that especially the iron(II) system can produce high-density polyethylene in good yields when bulky ortho-substituted aryl groups are attached to the imine nitrogens. The new catalysts have polymerization activities comparable to, or even higher than, those of metallocenes under similar conditions. They exhibit further great potential for controlling polymer properties by external parameters such as pressure and temperature.

Most recently, Grubbs' group demonstrated that some neutral salicylaldiminato nickel(II) complexes, whose skeleton structure appears as **1b** in Fig. 1, show catalytic activities rivaling those of the diimine complexes [13]. This potentially opens the door to a new class of catalysts as the active sites derived from these nickel complexes are neutral, thus reducing the ion-pairing problems encountered in the current catalysts.

Theoretical studies have been carried out on all the late-transition-metal catalysts **1a** [14–27], **1b** [28], and **1c** [29–32] in Fig. 1. It is not the objective here to review all the computational results. We shall instead discuss the general mechanistic insight that has been gained from the theoretical studies with the main emphasis on Brookhart's diimine catalysts. The experimental work on late-transition-metal olefin polymerization catalysts was reviewed recently by Ittel et al. [33].

Similarly to the early-metal-based systems, the late-metal complexes can yield high-molecular-weight polymers. Moreover, they can lead to polyolefins with different microstructures, depending on the catalysts

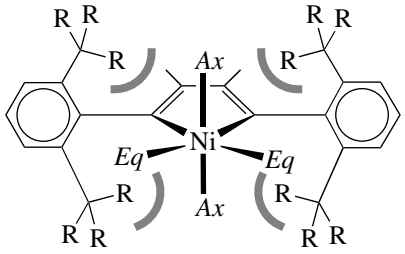

Fig. 3. Axial (*Ax*) and equatorial (*Eq*) coordination sites of the metal center and their potential steric interactions with the bulky substituents.

and the reaction conditions (temperature, olefin pressure) [33, 38].

In the present account, we describe how it is possible to model alkene homopolymerization in processes catalyzed by late-transition-metal complexes in such a way as to predict the influence of the catalyst structure and the reaction conditions (temperature and olefin pressure) on the polyolefin microstructure.

Recently, hyperbranched polymers were obtained [33–40] in the polymerizations of simple monomers such as ethylene and linear α-olefins, catalyzed by Ni- and Pd-diimine catalysts [1, 3, 33]. Branches in these polyolefins form as a result of fast chain isomerization reactions. The topology of the polymers is strongly affected by the olefin pressure: under low pressure, highly branched structures are obtained, whereas high pressure gives rise to structures with linear side chains. Interestingly, in the polymerization catalyzed by Pd diimine complexes, the average number of branches is pressure independent, while for the Ni-based system it is strongly affected by the pressure. Branching in olefin polymerization catalyzed by diimine complexes can be controlled also to some extent by the polymerization temperature and the substituents on the catalyst. Recently, another late-transition-metal catalyst was shown to exhibit similar branching features: in the polymerization processes catalyzed by a neutral Ni–anilinotropone complex, polymer branching can be controlled by a variation in temperature and pressure [41].

Quantum chemistry has established itself as a valuable tool in the studies of polymerization processes [42, 43]. However, direct quantum chemical studies on the relationship between the catalyst structure and the topology of the resulting polymer, as well as on the influence of the reaction conditions, are not practical without the aid of statistical methods. We have to this end proposed a combined approach in which quantum chemical methods are used to provide information on the microscopic energetics of elementary reactions in the catalytic cycle, which is required for mesoscopic stochastic simulations of polymer growth [42]. A stochastic approach makes it possible to discuss the effects of temperature and olefin pressure.

The major goal of this study was to understand the factors controlling polyolefin branching and the relationship between the catalyst structure, temperature, pressure, and the polyolefin topology. The DFT calculations were carried out for the elementary reactions in the polymerization of ethylene and propylene catalyzed by Pd-based diimine catalysts [24, 25] and the ethylene polymerization catalyzed by the Ni-anilinotropone catalyst [45]. The polymer growth in these processes was modeled by a stochastic approach [44–46]. Further, the model simulations were performed, by systematically changing insertion barriers, to model the influence of catalyst, beyond the diimine systems [46].

1. STERIC CONTROL OF MOLECULAR WEIGHT

We discuss in this section how steric bulk can be used to increase molecular weight by enhancing the rate of insertion (Fig. 2, stage (b)) and decrease the rate of termination. We shall demonstrate this point by first discussing the barriers of insertion/termination for the generic diimine system (HN=C(H)–C(H)=NH)M–R^+ in which we have replaced the aryl rings of **1a** in Fig. 1 with hydrogens. These barriers will be compared to those obtained from calculations on the full system in order to gauge the influence of steric bulk. The uptake of an ethylene molecule by (HN=C(H)–C(H)=NH)Ni$C_3H_7^+$, stage (**a**) in Fig. 2, is exothermic [22] by 19.9 kcal/mol and results in the formation of a π-complex in which the ethylene molecule is situated in an axial position above the N–Ni–N coordination plane, **3a** in Fig. 4. The π-complexation energy is higher than that for early d^0 transition metal complexes because of the additional metal-to-olefin back donation. In fact, the π-complex is so stable that, according to experimental studies [33], it becomes the resting state for the catalytic system. For (HN=C(H)–C(H)=NH)Pd$C_3H_7^+$, stage (b) in Fig. 2, one finds [24] a similar ethylene complexation energy of 18.8 kcal/mol.

Insertion of ethylene into the Ni–C bond in **3a** leads to the alkyl complex **4a** via the transition state TS [**3a**–**4a**] with a barrier [22] of 17.5 kcal/mol relative to **3a** (Fig. 4). It is worth noting that, in TS[**3a**–**4a**], both ethylene and the α-carbon of the growing (propyl) chain are situated in the N–Ni–N plane. For the corresponding palladium complex the insertion barrier [24] is somewhat higher at 19.9 kcal/mol.

The termination process of Fig. 2, stage (b) takes place from **3a** by transfer of a β-hydrogen on the growing chain to a carbon on the incoming ethylene monomer. The result (**5a** in Fig. 4) is a new (ethyl) growing chain and a complexed olefinic (propylene) unit made up of the old (propyl) growing chain. The olefinic unit might subsequently dissociate, thus giving rise to chain termination. The transition state for this process TS[**3a**–**5a**] has a barrier [22] of 9.7 kcal/mol. It is important to note that, in TS [**3a**–**5a**] (Fig. 4), we have two groups in the axial position over and below the

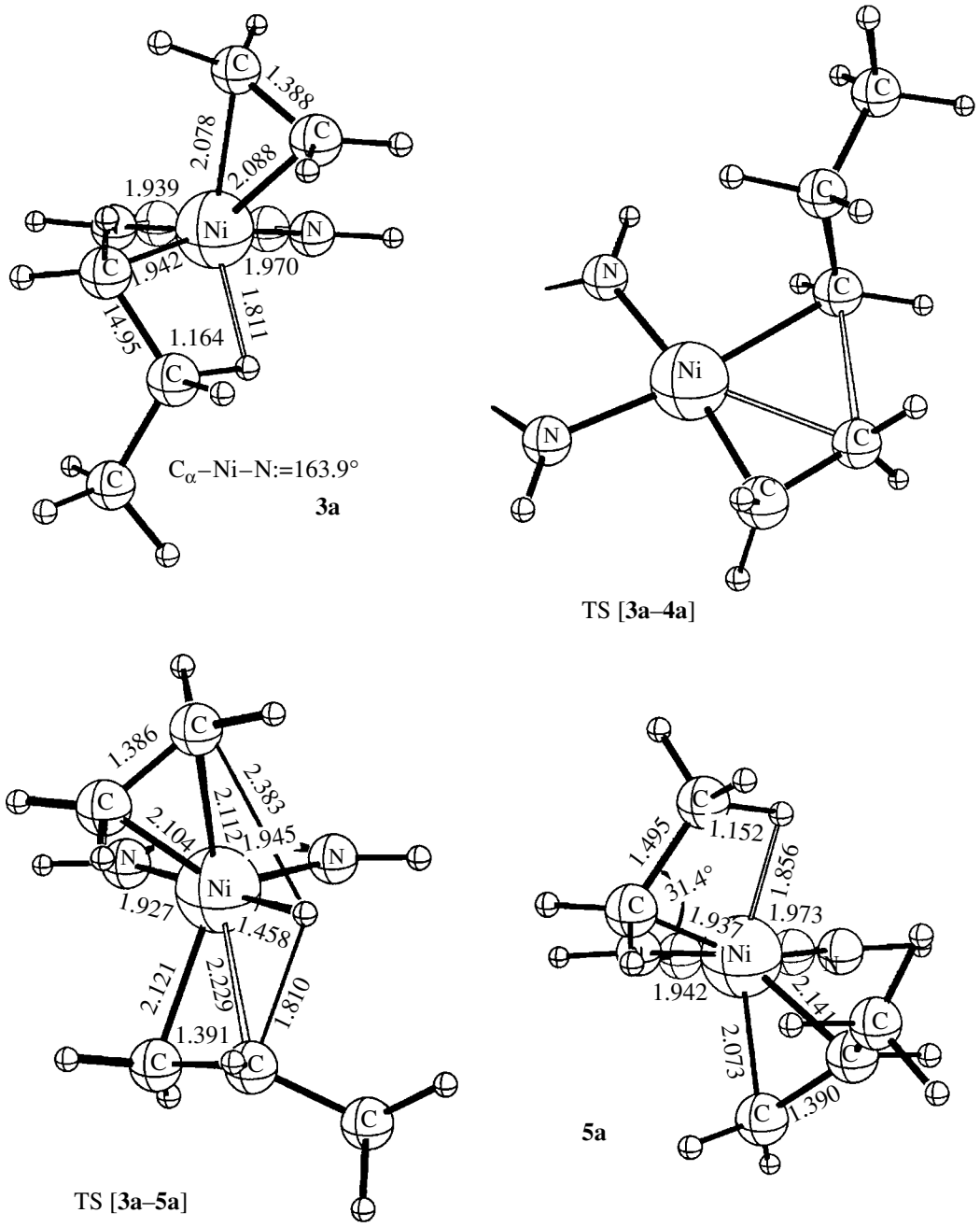

Fig. 4. Structures resulting from ethylene insertion and chain termination due to the generic catalyst (HN=C(H)–C(H)=NH)Pd$C_3H_7^+$. Ethylene complex (**3a**), insertion transition state (TS [**3a**–**4a**]), termination transition state (TS [**3a**–**5a**]), new olefin product from termination process (**5a**).

N–Ni–N coordination plane (see also Fig. 3). One group is the incoming ethylene and the other is the α-carbon of the growing (propyl) chain.

It follows from our discussion so far [22] that, for the generic catalyst, termination has a much lower barrier than insertion. Thus, (HN=C(H)–C(H)=NH)Ni$C_3H_7^+$ is not going to be an efficient olefin polymerization catalyst. Rather, stage (a) in Fig. 2 will at best be able to produce small oligomers of ethylene. This is in line with the experimental observation [33] that only diimines with bulky substituents are able to function as polymerization catalysts, whereas less encumbered systems work as oligomerization catalysts.

We shall now discuss how the introduction of steric bulk influences both insertion and termination. Our discussion will be based on calculations [23] involving **1a** in Fig. 1 in which M = Ni, R = Pr, and R' = H. We shall

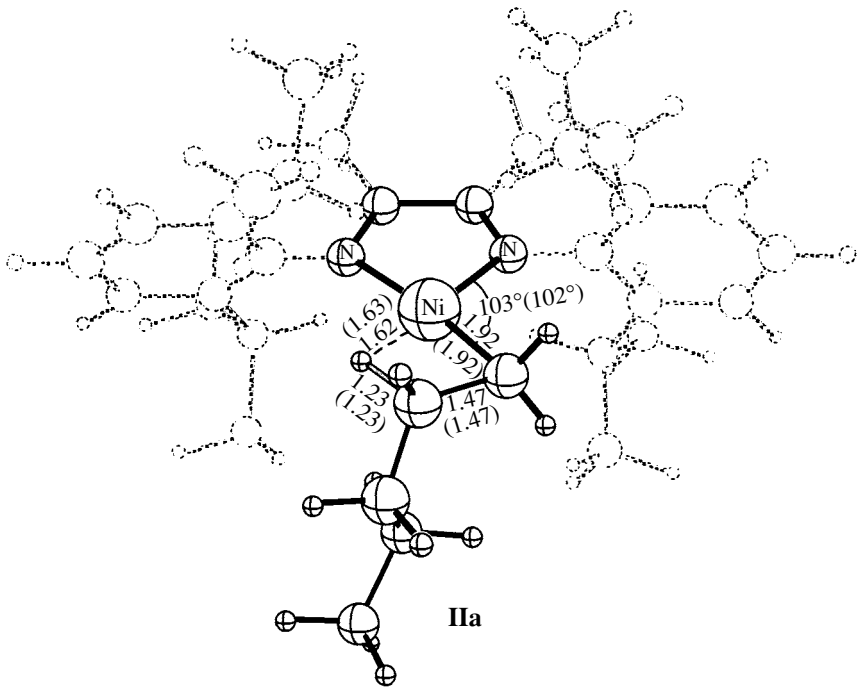

Fig. 5. QM/MM representation of structure **IIa**.

label the different species involved by Roman numerals to distinguish them from the corresponding generic systems labeled by Arabic numerals. In the actual calculations on **Ia** (or **IIa**), use was made of a combined quantum mechanical (QM) and molecular mechanical (MM) scheme [23] in which the core ((HN=C(H)–C(H)=NH)$NiC_3H_7^+$) was represented by QM and the remaining part by MM. Quite similar calculations were carried out by Morokuma et al. [19].

The uptake of olefin by **IIa** (Fig. 5) leads to the ethylene complex **IIIa** in Fig. 6 with a complexation energy [23] of 14.7 kcal/mol. The ethylene complexation energy is reduced compared to the generic system **3a** by 5.2 kcal/mol. This is understandable since the ethylene molecule in **IIIa** sits in one of the axial positions and thus is encumbered sterically by the bulky phenyl groups (Figs. 3, 6). Further studies have shown that the uptake energy can be influenced by a few kcal/mol by changing the substituents R and R' on **1a** in Fig. 1. It has also been demonstrated that the steric bulk on the diimine nitrogens gives rise to a free energy of activation barrier for the uptake due to entropic effects as the ethylene monomer has to approach a narrow channel in order to bind to the metal [26].

The subsequent insertion of ethylene into the Ni–C bond transforms **IIIa** into the pentyl complex **IVa** via the insertion transition state TS [**IIIa**–**IVa**] in Fig. 6. However, it is interesting to note that the barrier of insertion has been reduced from 17.5 kcal/mol for the generic system (TS [**3a**–**4a**]) to 13.2 kcal/mol for the real system [23] (TS [**IIIa**–**IVa**]). The reduction is not so much due to a change in the relative energies of the transition states since both the monomer and the α-carbon of the growing chain are situated in the N–Ni–N coordination plane (Fig. 6), where they are relatively unencumbered by the bulky phenyl groups. Instead, it is the steric destabilization of the **IIIa** resting-state relative to **3a** that is responsible for the reduction in the insertion barrier for the real system. Thus, by introducing steric bulk, one is able to enhance the polymerization activity of the Brookhart based Ni(II)-diimine complexes. Similar conclusion have been reached for the homologous Pd(II) systems [1–4]. However, the effect is not as pronounced as the steric congestion around the palladium center is less pronounced owing to the longer Pd–N bonds.

It is worth noting that the calculated insertion barrier [23] of 13.2 kcal/mol recently has been confirmed by Brookhart et al. [33] with an experimental estimate of 12.0 kcal/mol. A similar good agreement between theory and experiment has also been obtained for the palladium [27] system. The termination process leading from **IIIa** over TS [**IIIa**–**Va**] to **Va** by the transfer of a β-hydrogen on the growing chain to a carbon on the incoming ethylene monomer is calculated to have a barrier of 18.6 kcal/mol. This is a substantial increase compared to the generic system with a barrier (TS [**3a**–**5a**]) of 9.7 kcal/mol. The increase can be understood by observing in Fig. 7 that the transition state TS [**IIIa**–**Va**] has the ethylene molecule in one axial position and the α-carbon of the growing chain in the other. It is thus understandable that introducing bulky aryl groups considerably destabilizes TS [**IIIa**–**Va**] compared to TS

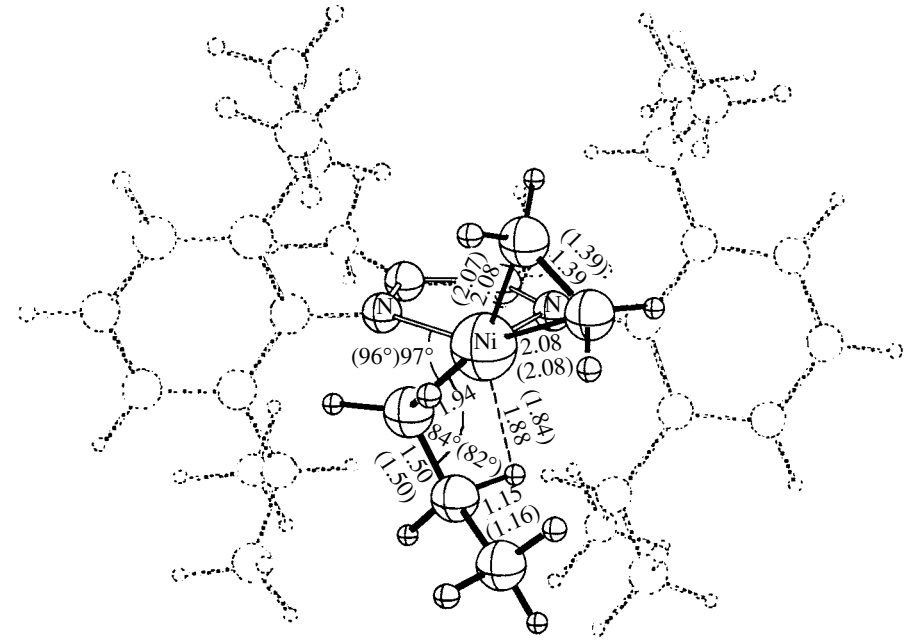

IIIa

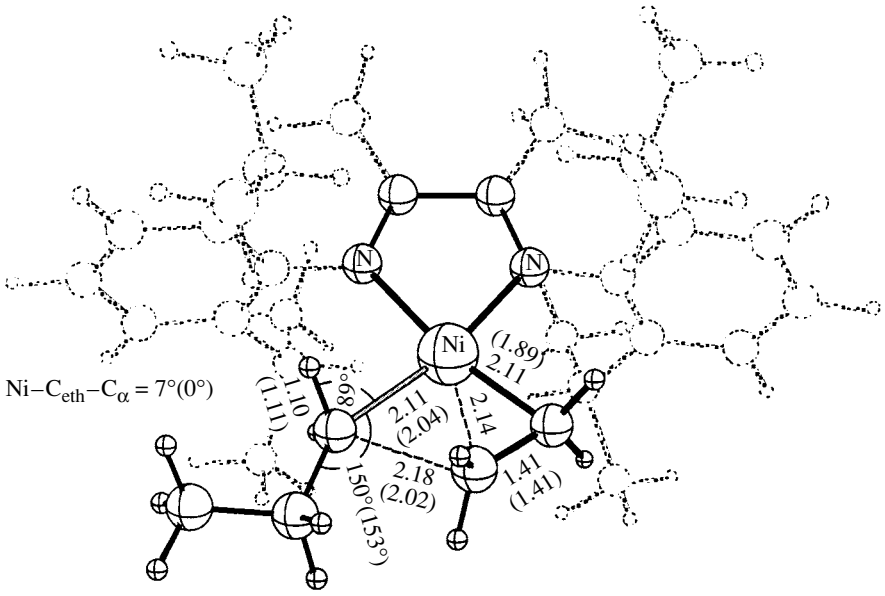

TS [**IIIa–IVa**]

Fig. 6. Ethylene complex (**IIIa**) and insertion transition state TS [**IIIa–IVa**] for the polymerization process involving **1a** (or **IIa**).

[**3a–5a**] with the result that termination becomes less feasible than propagation for the real system.

The discussion here illustrates that it should be possible by gradually increasing the size of the substituents on the diimine nitrogen atoms to proceed from catalysts for oligomerization to polymerization catalysts. For the recent Grubbs catalyst [13] (**1b** in Fig. 1), steric bulk is also required [28] to obtain high-molecular-weight polymers. For the Fe(II) and Co(II) catalysts [11, 12] with tridentate pyridine diimine ligands (**1c** in Fig. 1), steric bulk is required to destabilize the resting state in the form of an olefin complex and lower [29, 30] the barrier of insertion sufficiently. The Fe(II) system seems further to carry out insertion and termination on energy surfaces with different [29, 32] spin multiplicity.

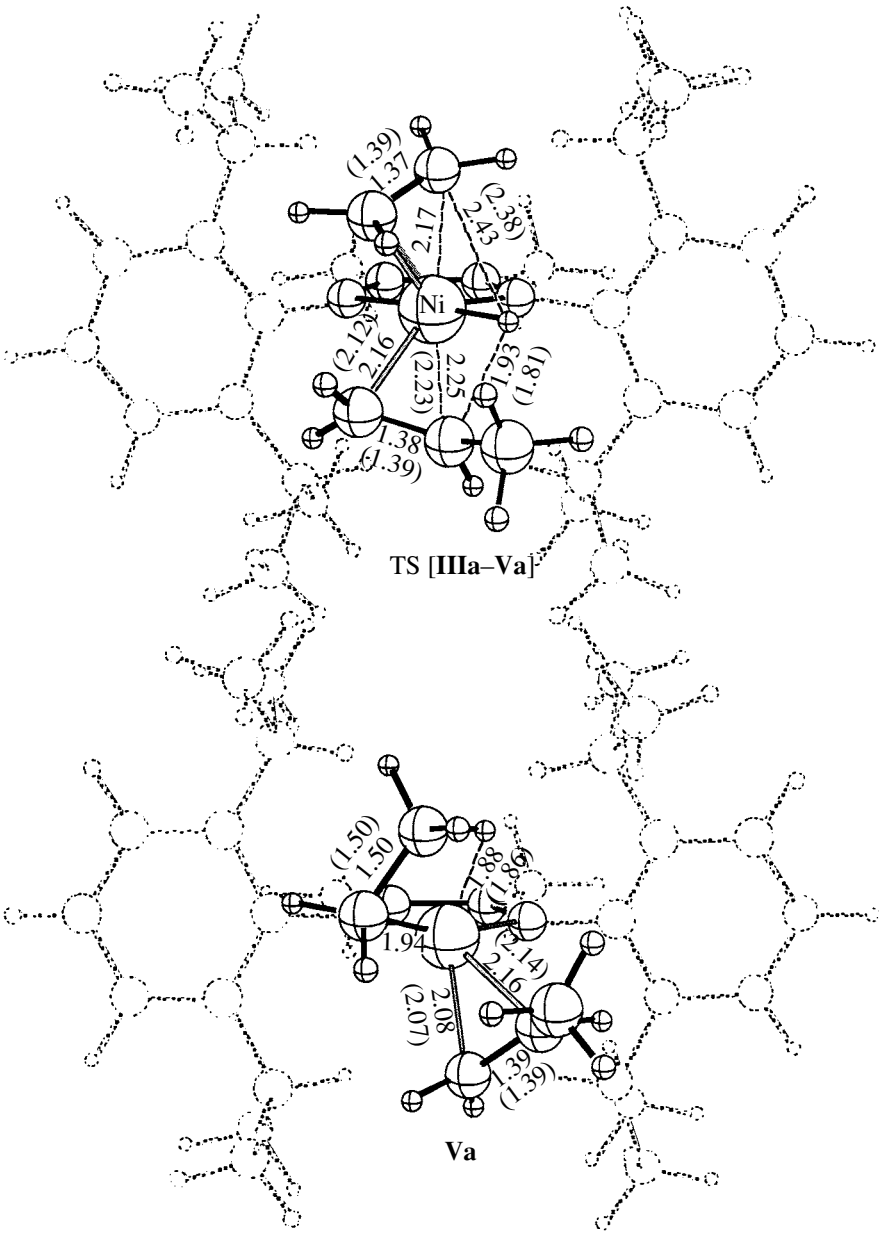

Fig. 7. Transition state TS (**IIIa**–**Va**) and product **Va** process involving hydride transfer process from original ethylene complex **IVa**.

2. CONTROL OF THE POLYMER TOPOLOGY

The third process in Fig. 2 involves the possible isomerization (branching) of a growing chain. The isomerization is mediated first by the migration of a β-hydrogen on the alkyl chain of **IIa** to the metal center, thus producing a hydrido olefin complex. The β-hydrogen elimination is followed by a 180° rotation of the olefin unit and a subsequent insertion of the olefin into the M–H bond, resulting in an isomerization (branching) of the growing chain. The principle is illustrated by the isomerization of the *n*-propyl chain in **IIa** via the transition state TS [**IIa**–**VIa**] in Fig. 8 to produce the isopropyl complex **VIa**. The internal barrier (relative to **IIa**) for the process is 15.3 kcal/mol [23]. For the generic (C(H)=NH)Ni(n-C_3H_7)$^+$ system, the isomerization barrier is [22] somewhat lower at 12.8 kcal/mol. This is understandable since the olefin unit has more space for its rotation.

In the case of the Pd diimine catalyst, the isomerization process has a barrier of 5.8 kcal/mol [24] for the generic system and 6.1 kcal/mol [33] for the real catalyst. The lower barrier is a result of the longer Pd–N distance (compared to the Ni–N bond length), which provides space for rotation of the olefin unit, even when the diimine nitrogens are attached to bulky substituents.

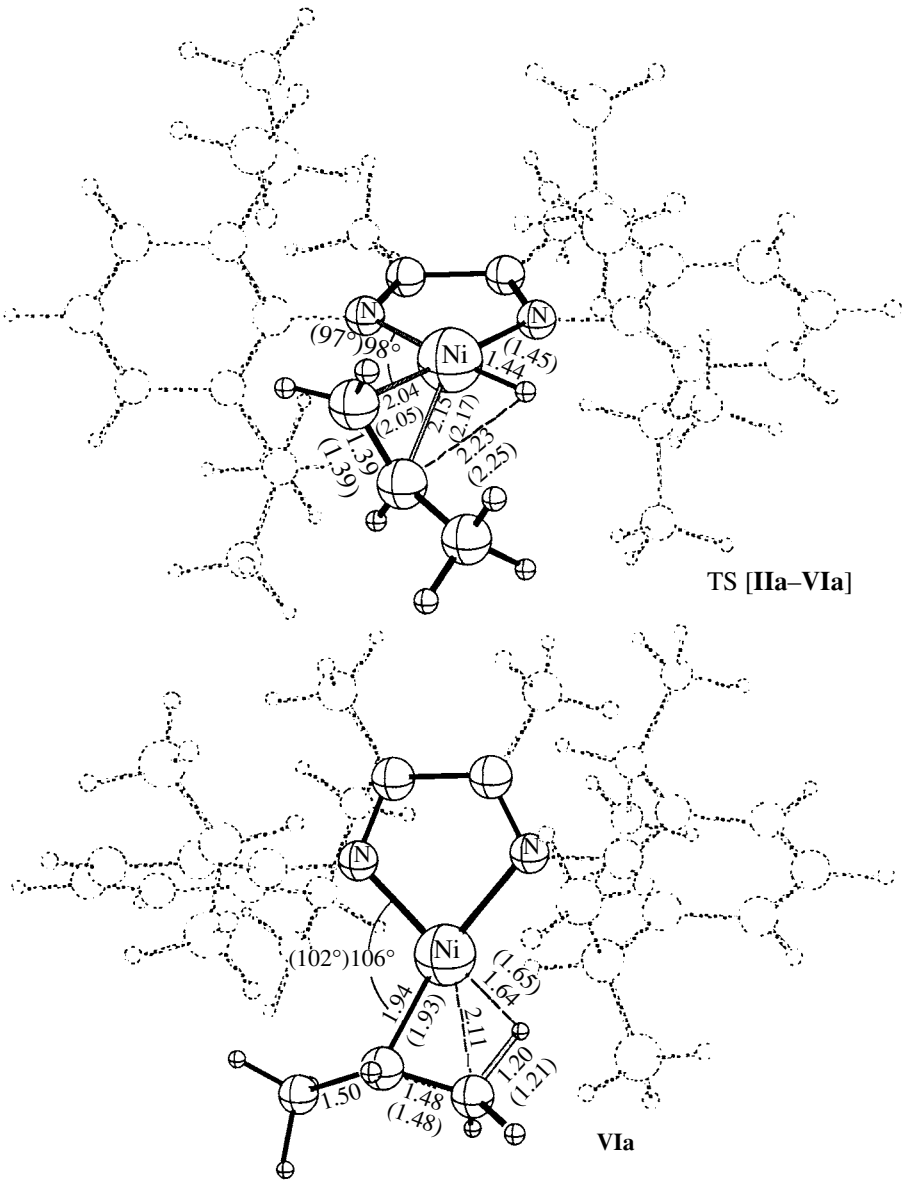

Fig. 8. Transition state TS [**IIa–VIa**] and product **VIa** from the isomerization of **IIa**.

The fact that the internal barrier of isomerization is much lower for the palladium than for the nickel system makes the former a more likely candidate for producing branched polymers. We shall in the following illustrate how palladium catalysts can be used to produce different branched structures by changing the steric bulk around the metal center. The principle will be illustrated in connection with the polymerization of propylene and ethylene.

2.1. Modeling the Polyolefin Branching

Scheme 1 presents the mechanism of propylene polymerization catalyzed by late-metal catalysts. In this process, the resting state of the catalyst is an olefin π-complex, **A**, from which the polymer chain may grow via 1,2-(**RA**) or 2,1-insertion (**RB**). Both insertion paths introduce one methyl branch. The "chain straightening" isomerization reaction (**RC**) is responsible for a removal of a branch; this isomerization reaction may follow the 2,1-insertion. However, the isomerization reactions may also elongate branches, when they proceed in the opposite direction (**RD**, **RE**, etc.). Another isomerization reaction which may follow the 1,2-insertion introduces an additional methyl branch and also may proceed further (**RF**, **RG**, etc.). Thus, in the polymerization cycle, many different alkyl species are present (**B–F**), in which the metal atom forms a bond with primary, secondary, or tertiary carbon atoms; each of them can capture a new monomer and give rise to a

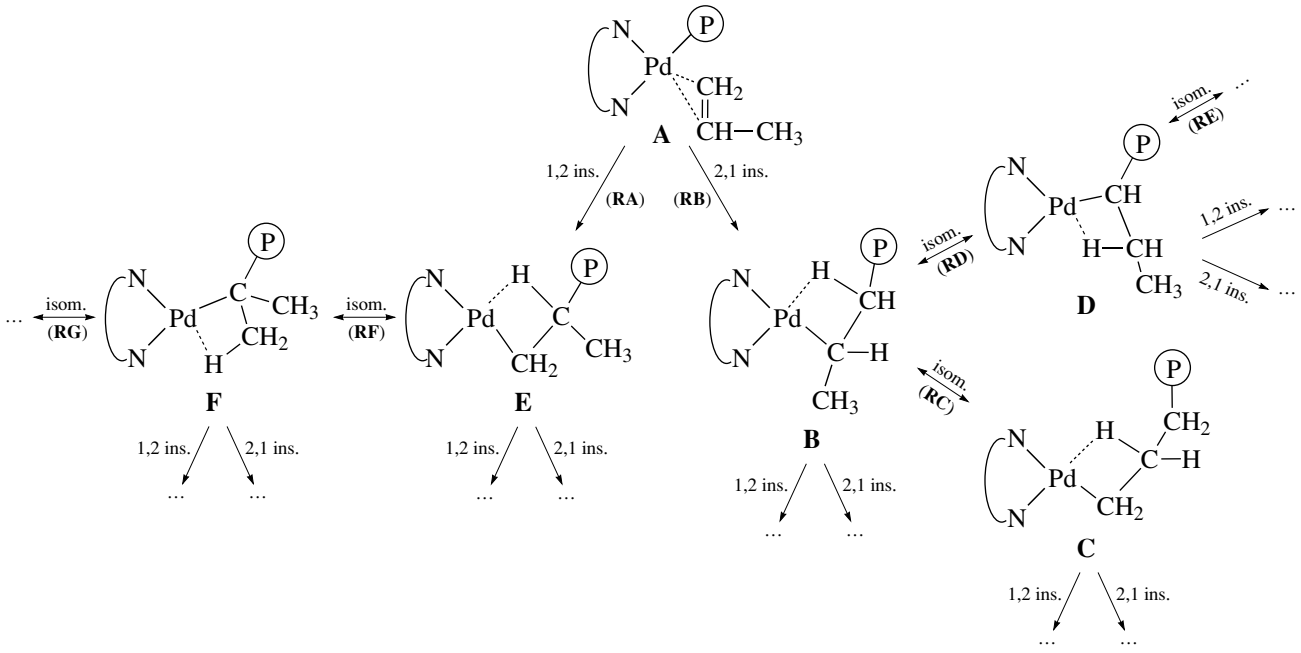

Scheme 1. Chain growth and isomerization reactions in the α-olefin polymerization catalyzed by Pd diimine catalyst.

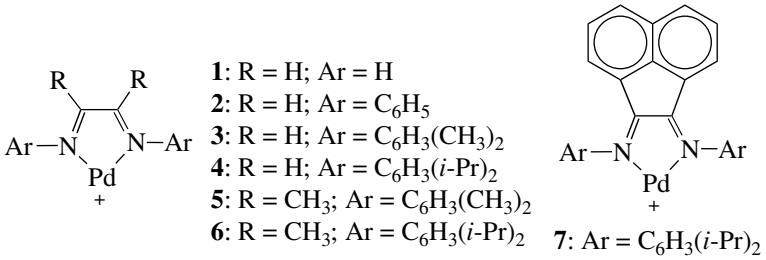

Scheme 2. Model and "real" Pd(II)-based diimine catalysts.

subsequent insertion. Thus, in order to understand the influence of the catalyst and reaction conditions on the polymer microstructure, one must consider all these elementary reactions.

2.2. Energetics of Elementary Reactions and Relative Stability of Isomers

In two recent papers [24, 25], we reported the results of computational studies on the elementary reactions in the ethylene and propylene polymerization catalyzed by Pd-based diimine catalysts with different substituents (Scheme 2). Comparison of the results for the model catalysts (**1**) and the real systems (**2**–**7**) of Scheme 2 makes it possible to separate the electronic and steric effects. The energetics of the elementary reactions in the catalytic cycle obtained from the calculations for **7** in Scheme 2 is summarized and compared with experimental data [47–49] in Fig. 9. Similar studies were performed [35] for the ethylene polymerization with the Ni-anilinotropone complex.

2.2.1. Relative stability of isomeric alkyl complexes and the olefin π-complexes. The calculations were performed for the isomeric propyl and butyl complexes. Two general trends can be observed [24, 25, 45] for both diimine and anilinotropone complexes: (i) the more branched the alkyl, the more stable the corresponding β-agostic complex; (ii) the steric bulk on the catalyst has little effect on the relative stability of the alkyl complexes. There are two opposing factors determining the stability of alkyl complexes: (i) the stability of free alkyl radicals, increasing for more branched systems; (ii) the energy of binding of the radicals, decreasing for more branched alkyls [25]. As a result, the energy order of isomeric alkyl complexes resembles the energy order of the alkyl radicals, with smaller energy differences between them than between the free radicals.

For the model catalysts **1** in Scheme 2, the olefin π-complexes with branched alkyls are more stable than with the linear ones [25]. This electronic preference is strongly affected by the steric bulk on the catalyst owing to an interaction between the alkyl group and the catalyst substituents [25]. Thus, for the most bulky real catalysts, the π-complexes with linear alkyl have lower energy. This is true for both ethylene and propylene complexes. A similar effect was observed for both the diimine and anilinotropone systems [24, 25, 45]. The presence of the steric bulk also affects the olefin complexation energies and the relative stability of ethylene and propylene complexes. This has been discussed in details in [25].

2.2.2. Olefin insertion barriers, 1,2- vs. 2,1-propylene insertion. Comparing the systems with isomeric alkyls, the olefin insertion barriers increase from the systems with primary alkyl to those with tertiary alkyl [24]. As a result, the insertion from the tertiary π-complexes practically does not happen. In the case of the real Pd diimine systems, the TS for the secondary ethylene insertion has slightly higher energy than the primary TS. The computed value of 0.5 kcal/mol is slightly lower than the experimental result (1 kcal/mol, Fig. 9).

For the generic catalyst, the 2,1-insertion of propylene is preferred by ~2 kcal/mol over the 1,2-insertion. The origin of this preference was discussed in details in [24]. The propylene 1,2-insertion TS is hardly affected by the steric bulk [25]. However, the TS for the propylene 2,1-insertion is strongly destabilized owing to a repulsion between the methyl group of propylene and the catalyst substituents [25]. As a result, in the real systems, the 1,2-insertion becomes preferred. As we will discuss later, this is of great importance for the branching control in the propylene polymerization.

2.2.3. Chain isomerization barriers. In the case of Pd-diimine catalyst, the isomerization barriers (5.5–8.0 kcal/mol) are substantially lower than the insertion barriers (17.5–18.5 kcal/mol) [24, 25, 34, 47–49]. The difference between the isomerization and insertion barriers is substantially larger than that for the corresponding Ni complexes, for which the isomerization barriers are higher by approximately 5–8 kcal/mol and the insertion barriers are lower by 4–5 kcal/mol [18, 19, 22, 24]. As we will show later, this is responsible for a difference in the pressure effect on the branching numbers observed for Ni- and Pd-based systems [46].

The energetics of the isomerization reactions is determined by the stability of the alkyl complexes discussed earlier. We would like to point out only that, as a result, the isomerization going from primary to secondary carbon is always energetically favored. Also, the secondary C ⟶ secondary C isomerization reactions usually have lower barriers than the secondary C ⟶ primary C isomerizations. This implies a fast walking along the polymer chain.

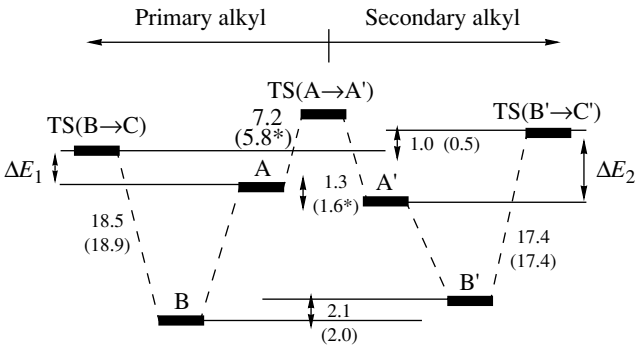

Fig. 9. Energetics (in kcal/mol) of the chain growth and chain isomerization reactions in the ethylene polymerization catalyzed by the Pd-diimine complex **7** (see Scheme 2). The experimental and theoretical (in parentheses) values are presented. The calculated energies for the chain isomerization reactions (marked with *) were obtained from the model catalyst **1**.

2.3. Stochastic Simulations of the Polyolefin Growth

The outcome of the complex polymer growth and branching in Scheme 1 is best modeled by the kind of stochastic simulations [44] described in the following. The outcome of such simulations are predictions about the polymer structures. A few initial steps in a typical simulation are presented in Fig. 10.

Initially, one carbon atom (a methyl group) is attached to the metal of the catalyst (**A** in Scheme 1). In the first step, it will capture and insert a propylene molecule via either the 1,2- or 2,1-insertion route. Thus, one of these insertion events is stochastically chosen; this choice, however, is not totally random but weighted by the probabilities of the two reactions. Here, the relative probabilities are proportional to the relative rates. Now, if one assumes that the 1,2-insertion has happened in the first step, the isobutyl group is attached to the catalyst (**B**) after insertion. At this stage, four different elementary events are possible: two alternative insertion routes (1,2- and 2,1-) followed by the capture of olefin, the termination reaction, and the isomerization reaction that would lead to a *tert*-butyl group attached to the metal center. If, for instance, the 2,1-insertion happened, a heptyl group would be attached to the catalyst by its secondary carbon atom (**C**); thus, five reactive events would be possible (two insertions, a termination, and two isomerizations); one of them would be stochastically chosen in a next step, etc. In the stochastic model, one assigns different probabilities for similar events starting from and/or leading to structures with a carbon atom of different character being attached to a metal. For example, the 1,2-insertion starting from a primary carbon is not equivalent to the 1,2-insertion starting from a secondary carbon. Similarly, the isomerizations starting from a primary, secondary, and tertiary carbon are not equivalent in general, and also the two isomerizations starting from a secondary carbon may be inequivalent, e.g., if one of

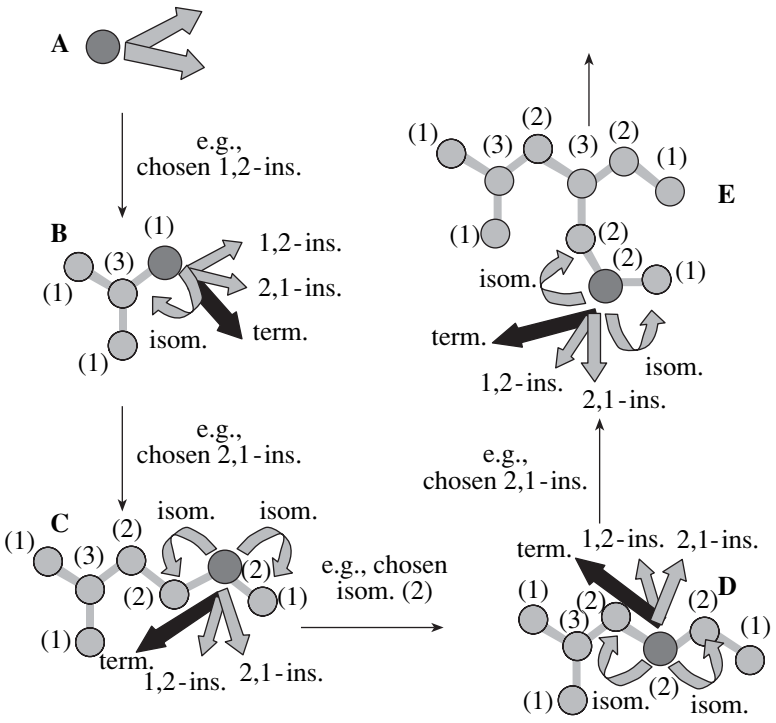

Fig. 10. Stochastic simulations. In the starting structure (**A**), one C atom is attached to the catalyst, and only two events are possible: propylene capture followed by the 1,2- or 2,1-insertion. For the structure **B**, four events are taken into account: isomerization to the tertiary carbon, 1,2- and 2,1-insertions, and a termination. For the structures **C**, **D**, and **E**, five events are considered: two isomerizations, two insertions, and a termination. The probabilities of these events are equal for the structures **C** and **E** (in both cases, two different isomerizations lead to a primary or secondary carbon at the metal) and different for the structure **D** (for which both isomerizations lead to the structure with a secondary carbon attached to the metal). For clarity, the numbers ((1), (2), and (3)) labeling different atom types (primary, secondary, and tertiary, respectively) are shown.

them leads to a primary and another to a secondary or tertiary carbon at the metal (as at stage **C** and **E**). In other words, one takes into account in this model three different 1,2-insertions, three different 2,1-insertions, three different terminations (each starting from 1°-, 2°-, and 3°-carbon), and nine different isomerizations (starting from and leading to 1°-, 2°-, and 3°-carbon).

It should be emphasized here as well that, at different stages, the absolute probabilities of equivalent events may be different, since they depend on the probabilities of all the other events (because of the probability normalization). For example, at the stages **C** and **D** in Fig. 10, the secondary carbon is attached to the metal, and five reactive events are possible. However, at the stage **C**, the isomerization reactions are inequivalent (one leads to the primary carbon and another to the secondary carbon), while at the stage **D** they are equivalent. As a result, the absolute probabilities of all the events at the stage **C** will differ from those at the stage **D**.

Scheme 3 summarizes the way in which the stochastic probabilities are generated from the rates of the different reactions. The basic assumption here is that the relative probabilities of elementary reactions at the microscopic level, π_i/π_j, are equal to their relative reaction rates (macroscopic), r_i/r_j. Thus, the relative reaction rates (Eq. (1) in Scheme 3) for all pairs of the considered reactive events together with the probability normalization condition (Eq. (2) in Scheme 3) constitute the system of equations that can be solved for the absolute probabilities of all the events at a given stage. With this assumption, one can use the experimentally determined reaction rates or the theoretically calculated relative rate constants, obtained from the energetics of the elementary reactions with the standard Eyring exponential equation. The Eyring equation introduces as well a temperature dependence of all the relative probabilities (as in Eq. (3) in Scheme 3).

Let us now have a closer look at three basic types of relative probabilities appearing in the model: for an isomerization vs. another isomerization, the 1,2-insertion vs. 2,1-insertion, and an isomerization vs. an insertion. The right-hand part of Scheme 3 summarizes the equations for the macroscopic reaction rates for the alternative reactive events starting from an alkyl complex β_0; let us assume that the secondary carbon atom is attached to the metal, so that two isomerization reactions have to be considered. The isomerization reactions are first-order in concentration of the initial alkyl complex, $[\beta_0]$ (Eqs. (6), (7) in Scheme 3). Thus, the relative probability for the two isomerizations (Eq. (3)) is given by the ratio of their rate constants, $k_{\text{iso, 1}}/k_{\text{iso, 2}}$ (as

Basic assumption:
relative probabilities (microscopic)
= relative rates (macroscopic):

$$\frac{\pi_i}{\pi_j} = \frac{r_i}{r_j} \quad (1); \qquad \sum_i \pi_i = 1 \quad (2)$$

e.g. isomerization vs. isomerization:

$$\frac{\pi_{\text{iso},1}}{\pi_{\text{iso},2}} = \frac{r_{\text{iso},1}}{r_{\text{iso},2}} = \frac{k_{\text{iso},1}}{k_{\text{iso},2}} \approx \exp\left(\frac{\Delta G^{\#}_{\text{iso},2} - \Delta G^{\#}_{\text{iso},1}}{RT}\right) \quad (3)$$

isomerization vs. insertion (1,2- or 2,1-):

$$\frac{\pi_{\text{iso},1}}{\pi_{\text{ins}}} = \frac{r_{\text{iso},1}}{r_{\text{ins}}} = \frac{k_{\text{iso},1}}{k_{\text{ins}} K_{\text{compl}} p_{\text{olefin}}} \quad (4)$$

1,2-insertion vs. 2,1-insertion:

$$\frac{\pi_{1,2\text{-ins}}}{\pi_{2,1\text{-ins}}} = \frac{r_{1,2\text{-ins}}}{r_{2,1\text{-ins}}} = \frac{k_{1,2\text{-ins}}}{k_{2,1\text{-ins}}} \quad (5)$$

etc.

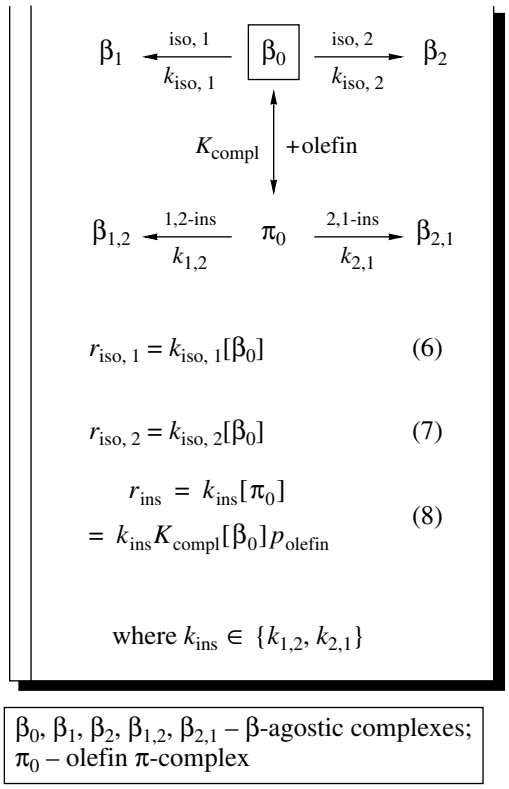

$$r_{\text{iso},1} = k_{\text{iso},1}[\beta_0] \quad (6)$$

$$r_{\text{iso},2} = k_{\text{iso},2}[\beta_0] \quad (7)$$

$$r_{\text{ins}} = k_{\text{ins}}[\pi_0] = k_{\text{ins}} K_{\text{compl}}[\beta_0] p_{\text{olefin}} \quad (8)$$

where $k_{\text{ins}} \in \{k_{1,2}, k_{2,1}\}$

β_0, β_1, β_2, $\beta_{1,2}$, $\beta_{2,1}$ – β-agostic complexes;
π_0 – olefin π-complex

Scheme 3. Basic equations used in the stochastic model.

equal to the relative rate, $r_{\text{iso},1}/r_{\text{iso},2}$), and at a given temperature, it can be calculated from the isomerization barriers $\Delta G^{\#}_{\text{iso},1}$ and $\Delta G^{\#}_{\text{iso},2}$, as in Eq. (3).

From alkyl complex β_0, the olefin can be captured to form the π-complex π_0 and inserted via the 1,2- or 2,1-insertion route. In the model applied here, we consider the olefin capture and its insertion as one reactive event; i.e., we assume a preequilibrium between the alkyl and olefin complexes, described by an equilibrium constant $K_{\text{compl}} = [\pi_0]/[\beta_0] = \exp(\Delta G_{\text{compl}}/RT)$. This corresponds to neglecting the barrier for the monomer capture. Such an approach is valid for the late-transition-metal complexes, e.g., the diimine catalysts studied in the present work, where the resting state of the catalyst is a very stable olefin π-complex [33] and the olefin capture barrier and the related π-complex dissociation barrier are much lower than the insertion barriers. This assumption allows one to speed up the simulation: otherwise, many olefin capture/dissociation steps, not important for the final result of the simulation, would occur before insertion takes place. It follows from the above considerations that the insertion rate is given by Eq. (8), and the equation for the isomerization vs. insertion relative probability (Eq. (4)) includes the isomerization and insertion rate constants, the equilibrium constant (K_{compl}), and the olefin pressure (p_{olefin}). Finally, the relative probability for the two alternative insertions is given by Eq. (5); it depends on the ratio of the two rate constants only.

It is important to emphasize here that the model in such a form allows one to simulate the influence of the reaction conditions. The temperature dependence of all the relative probabilities appears in the exponential expressions for the rate constants and the equilibrium constants. The olefin pressure influences the isomerization-insertion relative probabilities. As a result, both temperature and olefin pressure influence the values of the absolute probabilities for all the reactive events considered. In the following, use has been made of calculated reaction rates [27] to evaluate all stochastic probabilities, unless otherwise stated.

2.3.1. Ethylene polymerization catalyzed by Pd diimine catalyst. The simulations [46] performed for the ethylene polymerization catalyzed by the Pd-based diimine catalyst **7** (Scheme 2) with the theoretically determined energetics [33, 34] of elementary reactions gave the average branching number of 131 branches/1000 C. This is in reasonable agreement with the experimental value of 122 branches/1000 C [19] obtained for a closely related system **6** in Scheme 2. To further validate our model, we performed the simulations with the experimental values [47–49] of the reaction barriers and stabilities of intermediates (see Fig. 9). The value of 121 branches/1000 C was obtained, in very good agreement with experiment.

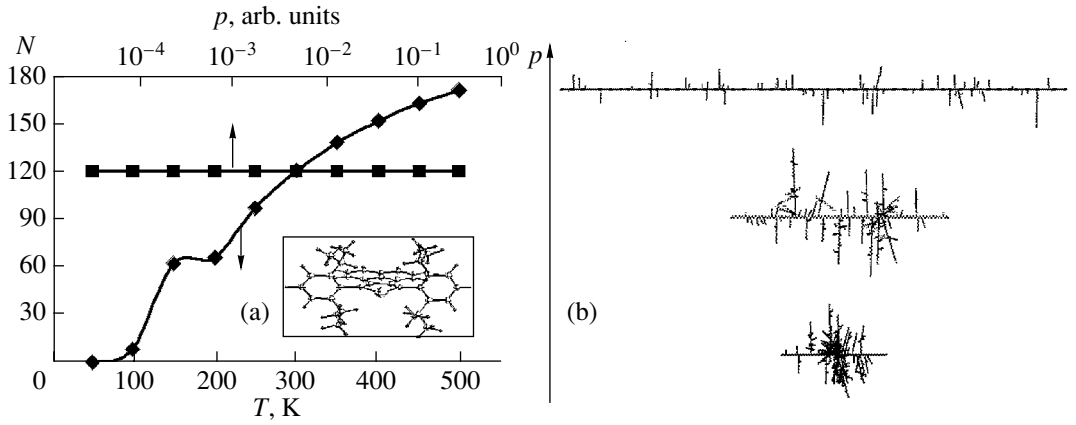

Fig. 11. The pressure and temperature dependence of the average number of branches (N) in the ethylene polymerization catalyzed by the Pd-based diimine catalyst **7** obtained from the stochastic simulations based on experimental energetics (a). The influence of pressure on the polymer topology (b); in each case, a chain of 1000 carbon atoms is shown and the main chain of the polymer is projected along the horizontal axis.

Figure 11 presents the temperature and pressure effects on the average number of branches. The results indicate an increase in the number of branches with an increase in temperature, in agreement with experimental observations [35–38]. This trend can be understood from the energetics of the catalytic cycle (see Fig. 10). The TS for secondary insertion is higher in energy (by 1 kcal/mol) than the TS for primary insertion. Thus, in the limit of $T = 0$ K, only primary insertions may occur, and with an increase in temperature, the fraction of secondary insertions increases.

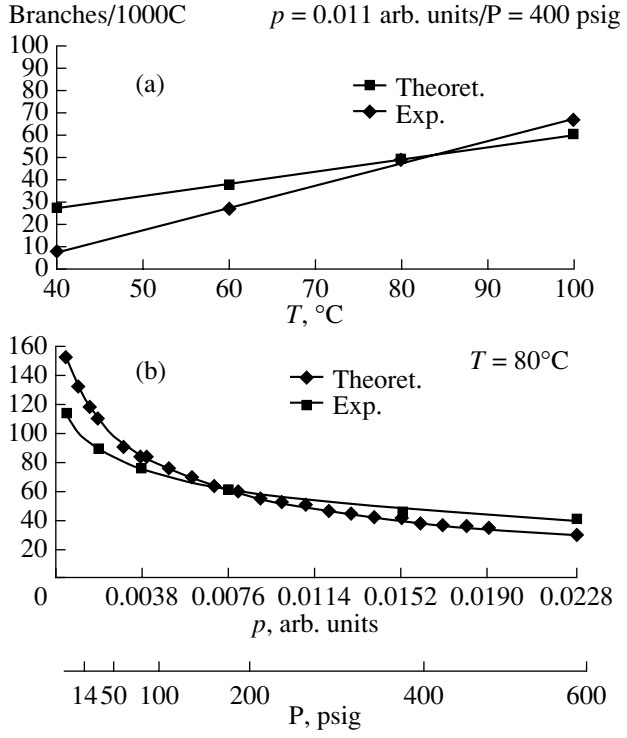

Fig. 12. The calculated and experimental temperature (a) and pressure (b) dependence of the average number of branches/1000C.

Figure 11 shows that, within a wide range of pressures, the simulations give a constant average number of branches. The microstructure of the polymer, however, is strongly affected by the pressure. Examples of the polymer structures obtained from the simulations are shown in Fig. 11. The polymers obtained at high pressures are mostly linear with a large fraction of atoms located in the main chain and with relatively short and mostly linear side chains. With a decrease in pressure, hyperbranched structures are formed. Both the pressure independence of the branching number and the pressure influence on the polymer topology are in agreement with experimental data for Pd catalysts [33, 35–38].

2.3.2. Propylene polymerization catalyzed by the Pd diimine catalysts. For the propylene polymerization catalyzed by the complexes **1**–**7** (Scheme 2), the simulations were performed [44] on the basis of the calculated energetics of the elementary reactions [24, 25]. For system **6** of Scheme 2, the calculated average number of branches is 238 br./1000 C, which is slightly larger than the experimental value of 213 br./1000 C. However, the temperature and pressure dependence of the number of branches and the polymer microstructure are in line with experimental observations [38]: (1) an increase in polymerization temperature leads to a decrease in the number of branches; (2) olefin pressure does not affect the branching number, but affects the topology, leading to hyperbranched structures at low p.

Further, the simulations confirm the experimental interpretation of the mechanistic details of the process with the catalyst **6** of Scheme 2 [38]: (1) both 1,2- and 2,1-insertions happen with the ratio being about 7 : 3; (2) there are no insertions at the secondary carbons; (3) most of the 2,1-insertions are followed by a chain straightening isomerization. Thus, for this catalyst, the

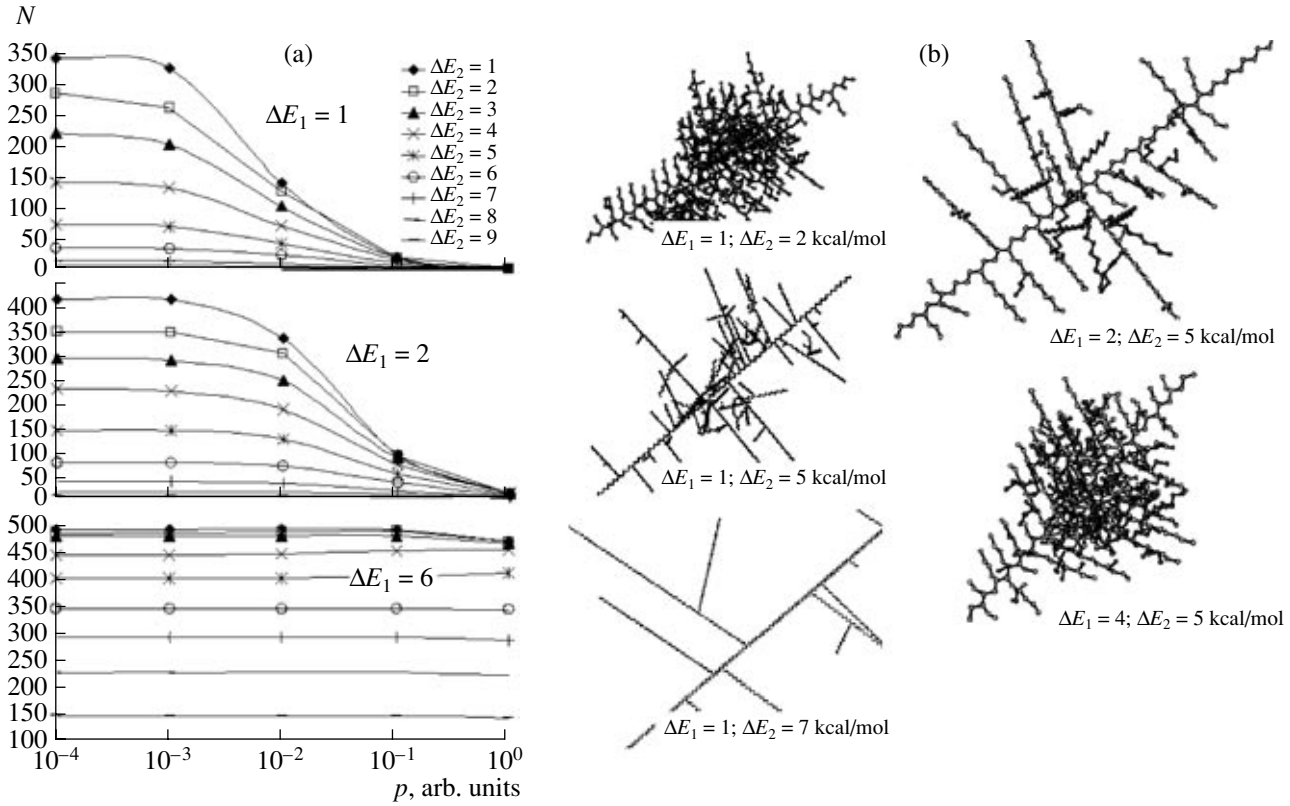

Fig. 13. The pressure dependence of the average number of branches obtained from the model stochastic simulations with different primary and secondary insertion barriers, ΔE_1, ΔE_2 (a), and examples of polymer topologies (b). Different atom shadings are used to mark different types of branches (primary, secondary, etc.).

total number of branches is controlled exclusively by the 1,2-/2,1-insertion ratio [44].

We would like to emphasize here that the branching of polypropylene is controlled by different factors than that of polyethylene [46]. In the case of ethylene, the primary/secondary insertion ratio is crucial, whereas in the propylene polymerization catalyzed by diimine catalysts, the ratio between the two alternative insertion pathways (1,2- and 2,1-) is more important [44]. As a result, an opposite temperature effect has been observed for ethylene (increase in branching number with T) and propylene (decrease in branching number with T).

2.3.3. Ethylene polymerization catalyzed by the Ni anilinotropone catalyst. The results of the simulations based on the DFT-calculated energetics [35] for the Ni-anilinotropone catalyst are presented in Fig. 12. The simulations reproduced [45] with reasonable agreement the experimental pressure and temperature dependence of the average number of branches [41]. The temperature dependence (increase in branching number with an increase in temperature) can be rationalized in a similar way as for diimine catalysts.

In addition, the stochastic simulations provided detailed information about the topology of the polyethylenes produced in these processes [45]. The results indicate that a variation in pressure affects the polymer topology more than a variation in temperature. In the low-pressure regime, the length of the branches increases and branch-on-branch structures are formed more often.

2.3.4. Model simulations—effect of catalyst variation. To model branching features of the ethylene polymerization processes catalyzed by different single-site catalysts, we performed a set of model simulations [46] in which the barriers for the primary and secondary insertions were systematically changed, ΔE_1, ΔE_2 = 1–9 kcal/mol (see Fig. 9). A change of the two insertion barriers corresponds to a change of the catalyst, as the processes catalyzed by different systems are characterized by different free energy profiles.

Figure 13 presents the pressure dependence of the average number of branches for different sets of insertion barriers. The curves of Fig. 13 can be understood when one notices that (i) in the limit of $p \longrightarrow \infty$ (cf. Eq. (1) of Scheme 3), the number of branches must be zero for each catalyst, as ethylene π-complexes would be formed immediately after the insertion and there would be no isomerization; (ii) in the limit of $p \longrightarrow 0$, chain walking would be infinitely fast compared to insertions (cf. Eq. (1)), and then the number of branches would be controlled exclusively by the ratio of primary vs. sec-

ondary insertions (i.e., the insertion/isomerization ratio would not play a role). Thus, in the low-pressure range, the curves of Fig. 13 converge to the average number of branches characteristic of a given pair of [ΔE_1, ΔE_2], while in the high-pressure regime they decay to zero. Consequently, for each catalyst, there exists a range of (low) pressure values for which the average number of branches is pressure independent. With an increase in the insertion barriers, this range extends towards high pressure values (see Fig. 13).

It may be concluded from the results of Fig. 13 that the faster the chain walking compared to insertions, the more extended the range of pressures for which the average number of branches is constant. This allows us to qualitatively explain the difference between the Pd- and Ni-based diimine catalysts. It is known that, for the Pd-diimine systems, the isomerization is much faster compared to insertion than for Ni complexes [18, 19, 22–24, 33]. As a result, for the Pd systems, the number of branches is constant in the experimental range of pressure values, while for the Ni complexes the number of branches depends on the pressure in this range (and would be pressure independent for much lower pressures). It should be pointed out that the above discussion is consistent with the kinetic arguments given by Guan et al. [35] for the Pd diimine catalyst. Finally, let us now discuss the influence of the pressure on the polymer topology. Figure 13 displays examples of the polymer structures obtained for different combinations of ΔE_1, ΔE_2, for $p = 0.0001$. Although all the structures of Fig. 13 are practically hyperbranched, the topology varies to a large extent. As we discussed earlier, in the low-pressure regime, the branching is controlled by the ratio of primary and secondary insertions. Thus, the difference between the barriers for the primary and secondary insertions controls the polymer topology. For small values of $\Delta E_{2,1} = \Delta E_2 - \Delta E_1$, branches are formed as a result of both the primary and secondary insertions with comparable probablilities. With an increase in $\Delta E_{2,1}$, the probability of secondary insertions decreases and insertions at the ends of branches happen more often; as a result, an increase in the length of linear segments can be observed.

3. CONCLUSIONS

We have presented a comprehensive review of our recent theoretical studies on alkene homopolymerization catalyzed by the late-transition-metal complexes. The results of these studies show that a combined DFT/stochastic approach can be successfully used to model the elementary reactions in the polymerization processes and the influence of the reaction conditions on the polyolefin branching. Such an approach makes it possible to understand the microscopic factors controlling the branching of polyolefins and explain the differences between the Pd and Ni catalysts. The results also demonstrate that a wide range of microstuctures can be potentially obtained from ethylene polymerization. Thus, a rational design of the catalyst producing the desired polymer topology should be possible.

ACKNOWLEDGMENTS

This work has been supported by the National Sciences and Engineering Research Council of Canada (NSERC) and the Petroleum Research Fund, administered by the American Chemical Society (ACS-PRF No. 36543-AC3). A.M. acknowledges a NATO Postdoctoral Fellowship. T.Z. thanks the Canadian government for a Canada Research Chair.

REFERENCES

1. Johnson, L.K., Killian, C.M., and Brookhart, M., *J. Am. Chem. Soc.*, 1995, vol. 117, p. 6414.
2. Johnson, L.K., Mecking, S., and Brookhart, M., *J. Am. Chem. Soc.*, 1996, vol. 118, p. 267.
3. Killian, C.M., Tempel, D.J., Johnson, L.K., and Brookhart, M., *J. Am. Chem. Soc.*, 1996, vol. 118, p. 11664.
4. Wilke, G., *Angew. Chem., Int. Ed. Engl.*, 1988, vol. 27, p. 185.
5. Sen, A. and Ta-Wang, L., *J. Am. Chem. Soc.*, 1982, vol. 104, p. 3520.
6. Eur. Pat. Appl. EP 121965.
7. Haggin, J., *Chem. Eng. News*, 1996, Feb. 5, p. 6.
8. Keim, W., *Angew. Chem., Int. Ed. Engl.*, 1990, vol. 29, p. 235.
9. Abecywickrema, R., Bennett, M.A., Cavell, K.J., Kony, M., Masters, A.F., and Webb, A.G., *J. Chem. Soc., Dalton Trans.*, 1993, p. 59.
10. Brown, S.J. and Masters, A.F., *J. Organomet. Chem.*, 1989, vol. 367, p. 371.
11. Small, B.L., Brookhart, M., and Bennett, A.M.A., *J. Am. Chem. Soc.*, 1998, vol. 120, p. 4049.
12. Britovsek, G.J.P., Bruce, M., Gibson, V.C., Kimberley, B.S., Maddox, P.J., Mastroianni, S., McTavish, S.J., Redshaw, C., Solan, G.A., Stromberg, S., White, A.J.P., and Williams, D.J., *J. Am. Chem. Soc.*, 1999, vol. 121, p. 8728.
13. Wang, C., Friedrish, S., Younkin, T.R., Li, R.T., Grubbs, R.H., Bansleben, D.A., and Day, M.W., *Organometallics*, 1998, vol. 17, p. 3149.
14. Dedieu, A., *Chem. Rev.*, 2000, vol. 100, p. 543.
15. Musaev, D.G., Froese, R.D.J., and Morokuma, K., *J. Am. Chem. Soc.*, 1997, vol. 119, p. 367.
16. Musaev, D.G., Svensson, M., Morokuma, K., Strömberg, S., Zetterberg, K., and Siegbahn, P., *Organometallics*, 1997, vol. 16, p. 1933.
17. Musaev, D.G., Froese, R.D.J., and Morokuma, K., *New J. Chem.*, 1997, vol. 22, p. 1265.
18. Froese, R.D.J., Musaev, D.G., and Morokuma, K., *J. Am. Chem. Soc.*, 1998, vol. 120, p. 1581.
19. Musaev, D.G., Froese, R.D.J., and Morokuma, K., *Organometallics*, 1998, vol. 17, p. 1850.
20. Musaev, D.G. and Morokuma, K., *Top. Catal.*, 1999, vol. 7, p. 107.

21. Von Schenck, H., Strömberg, S., Zetterberg, K., Ludwig, M., Akermark, B., and Svensson, M., *Organometallics*, 2001, vol. 20, p. 2813.
22. Deng, L., Margl, P., and Ziegler, T., *J. Am. Chem. Soc.*, 1997, vol. 119, p. 1094.
23. Deng, L., Woo, T.K., Cavallo, L., Margl, P., and Ziegler, T., *J. Am. Chem. Soc.*, 1997, vol. 119, p. 6177.
24. Michalak, A. and Ziegler, T., *Organometallics*, 1999, vol. 18, p. 3998.
25. Woo, T.K. and Ziegler, T., *J. Organomet. Chem.*, 1999, vol. 591, p. 204.
26. Woo, T.K., Blochl, P.E., and Ziegler, T., *J. Phys. Chem. A*, 2000, vol. 104, p. 121.
27. Michalak, A. and Ziegler, T., *Organometallics*, 2000, vol. 19, p. 1850.
28. Chan, M.S.W., Deng, L., and Ziegler, T., *Organometallics*, 2000, vol. 19, p. 2741.
29. Deng, L., Margl, P., and Ziegler, T., *J. Am. Chem.Soc.*, 1999, vol. 121, p. 6479.
30. Margl, P., Deng, L., and Ziegler, T., *Organometallics*, 1999, vol. 18, p. 5701.
31. Griffiths, E.A.H., Britovsek, G.J.P., Gibson, V., and Gould, I.R., *Chem. Commun.*, 1999, p. 1333.
32. Khoroshun, D.V., Musaev, D.G., Vreven, T., and Morokuma, K., *Organometallics*, 2001, vol. 20, p. 2007.
33. Ittel, S.D., Johnson, L.K., and Brookhart, M., *Chem. Rev.*, 2000, vol. 100, p. 1169.
34. Britovsek, G.J.P., Gibson, V.C., and Wass, D.F., *Angew. Chem., Int. Ed. Engl.*, 1999, vol. 38, p. 428 (and references therein).
35. Guan, Z., Cotts, P.M., McCord, E.F., and McLain, S.J., *Science*, 1999, vol. 283, p. 2059.
36. Cotts, P.M., Guan, Z., McCord, E.F., and McLain, S.J., *Macromolecules*, 2000, vol. 33, p. 6945.
37. Derek, P., Gates, S.J., Steven, A., *et al.*, *Macromolecules*, 2000, vol. 33, p. 2320.
38. McCord, E.F., McLain, S.J., Nelson, L.T.J., Arthur, S.D., Coughlin, E.B., Ittel, S.D., Johnson, L.K., Tempel, D., Killian, C.M., and Brookhart, M., *Macromolecules*, 2001, vol. 34, p. 362.
39. Boffa, L.S. and Novak, B.M., *Chem. Rev.*, 2000, vol. 100, p. 1479 (and references therein).
40. Mecking, S., Johnson, L.K., Wang, L., and Brookhart, M., *J. Am. Chem. Soc.*, 1998, vol. 120, p. 888.
41. Hicks, F.A. and Brookhart, M., *Organometallics*, 2001, vol. 20, p. 3217.
42. Rappe, A.K., Skiff, W.M., and Casewit, C., *J. Chem. Rev.*, 2000, vol. 100, p. 1435 (and references therein).
43. Angermund, K., Fink, G., Jensen, V.R., and Kleinschmidt, R., *Chem. Rev.*, 2000, vol. 100, p. 1457 (and references therein).
44. Michalak, A. and Ziegler, T., *J. Am. Chem. Soc.*, 2002, vol. 124, p. 7519.
45. Michalak, A. and Ziegler, T., *Macromolecules*, 2003, vol. 36, p. 928.
46. Michalak, A. and Ziegler, T., *Organometallics*, 2003, vol. 22, p. 2069.
47. Tempel, D.J., Johnson, L.K., Huff, R.L., White, P.S., and Brookhart, M., *J. Am. Chem. Soc.*, 2000, vol. 122, p. 6686.
48. Shultz, L.H. and Brookhart, M., *Organometallics*, 2001, vol. 20, p. 3975.
49. Shultz, L.H., Tempel, D.J., and Brookhart, M., *J. Am. Chem. Soc.*, 2001, vol. 123, p. 11539.